Green Chemistry

PAPER

View Article Online
View Journal | View Issue

Cite this: *Green Chem.*, 2021, **23**, 7016

Innovative methodology for marine collagen–chitosan–fucoidan hydrogels production, tailoring rheological properties towards biomedical application

Duarte Nuno Carvalho, [a,b] Cristiana Gonçalves,[a,b] Joaquim Miguel Oliveira, [a,b] David S. Williams,[c] Andrew Mearns-Spragg,[c] Rui L. Reis[a,b] and Tiago H. Silva *[a,b]

Marine polymers such as collagen, chitosan, and fucoidan can be combined to form ionic-linked hydrogel networks towards applications in tissue engineering (TE). The use of greener approaches (as determined by green metrics – *E*-factor), including the absence of external chemical cross-linking agents, has advantages regarding the potential cytotoxicity. By tailoring the formulation of such an ionic-linked hydrogel, it is possible to fine-tune scaffold biofunctionality. In this study, a comparative study of composite hydrogels was accomplished, seeking to understand the correlation between polymer characteristics and physical behaviour to develop the applicability of this technology in soft-to-hard TE. Parameters such as polymer concentration, molecular weight, polymer-biomaterials bonds, biomaterial structural architecture, pore size, and mechanical rheological properties were directly correlated to the hydrogel's formulation. The results highlight that the formulation with greatest potential was the 3-component hydrogel (H_{12}, followed by H_{10}, H_{11}), due to its superior mechanical properties, making it suitable for cartilage TE. This research offers a valuable perspective on hydrogel formulation and a new processing methodology, as well as how tailoring the hydrogel composition influences mechanical behaviour to support selecting the best composition for tissue engineering applications.

Received 23rd June 2021,
Accepted 20th August 2021

DOI: 10.1039/d1gc02223g

rsc.li/greenchem

Introduction

Hydrogels are defined as cross-linked three-dimensional networks, able to absorb and retain substantial amounts of water.[1] These structures show several advantages: biocompatibility, hydrophilic nature, and 3D network structure fitting several biomedical applications (such as.: cell culture, tissue engineering, drug delivery, soft actuators.[2] Hydrogels can be prepared using reversible polymer connections (natural cross-linking), *via* ionic or hydrogen bonds, and by covalent bonds (chemical cross-linking agents).[3,4] However, even though chemical cross-linking can be used to stabilize hydrogels, by the capacity to increase the mechanical properties,[5] it may be environmentally advantageous to use natural cross-linking, as an alternative to chemical agents, to avoid concerns regarding cell cytotoxicity.[6,7] Thus, employing natural cross-linking to renewable and biocompatible blends of biopolymers is a green approach of exceptional value. In engineering materials, hydrogels can be prepared from a single polymer or a combination of natural or synthetic components, derived from various sources and being able to replicate the physical parameters of soft-to-hard tissues due to the specific limitations of self-repair capacity in some human tissues.[8,9]

To prepare these hydrogels, in the last decade, marine polymers have been considered an excellent natural alternative to their mammalian counterparts for new materials envisaging biomedical application (such as in articular cartilage therapies).[10,11] Besides, many marine biopolymers can be obtained from marine by-products (as fish skins and crustacean shells) and underused resources (as some species of seaweeds and jellyfish), following strategies of biomass valorization under the concept of circular economy. Likewise, due to the similarities of many of these biopolymers with the components of extracellular matrix (ECM) and their ability to incorporate bioactive functionalities to support cell viability and promote regeneration/restoration of damaged tissue,[12] its biomedical application has been increasingly studied. Furthermore, using marine resources such as collagen, chito-

[a]*3B's Research Group, I3B's – Research Institute on Biomaterials, Biodegradables and Biomimetics of University of Minho, Headquarters of the European Institute of Excellence on Tissue Engineering and Regenerative Medicine, AvePark 4805-017, Barco, Guimarães, Portugal*
[b]*ICVS/3B's – P.T. Government Associate Laboratory, Braga/Guimarães, Portugal*
[c]*Jellagen Limited, Unit G6, Capital Business Park, Parkway, St Mellons, Cardiff, CF3 2PY, UK*

san, and fucoidan avoids the risk of infections, immunogenicity, and minor regulatory limitation and refusals due to ethical issues (regarding social or religious concerns).[13,14]

Considering the properties of each body tissue, a combination of different materials in a hydrogel can be an important key to improve the biological and mechanical properties due to a single polymer lacking the requisite properties for the desired application.[15] The mechanical properties of hydrogels are directly correlated with their physical parameters such as porosity (mesh/pore size), polymer molecular weight, density, and type of cross-linking that occurs between the neighboring chains. These parameters are essential to predict the biomaterial behavior, particularly when being used for medical applications.[3,5] In rheological studies, the elastic shear modulus tested in biological materials should be tunable in the range of 0.01–0.1 kPa to 100 kPa to tolerate the adjustment of elasticity of a specific tissue. Materials with less than 0.1 kPa are suitable for soft tissues (as brain or fluid blood), while those with higher than 10 kPa are best suited to cartilaginous and bone tissues.[16,17] Regarding the mesh/pore size parameter, this plays an essential role in modulating cell migration, exchange of nutrients and waste products, whilst controlling the kinetic release of bioactive compounds when used in delivery systems.[3,12] However, the mesh size can also be a physical constraint. If the mesh/pore size is smaller than the cell size (typically between 7 μm and 15 μm), it can create an impediment to cell migration, endangering their survival, especially in systems that use encapsulated cells.[18,19] Moreover, hydrogels developed for application in articular cartilaginous areas should be able to deal with constant mechanical stress, typical of those zones subjected continuously to stretching and contracting movements.[20,21]

A simple, green chemistry technology for the fabrication of hydrogels based on natural resources is explored in this manuscript. The innovation of the present work is mainly related to the process used to blend the materials to achieve morphological and rheological properties, suited to tissue engineering applications, without chemical crosslinkers. In a previous work of our group we have already explored the combination of these marine polymers using cryo-environments (temperatures below zero) to promote the gelation between the polymers[20] but with this experimental work we aimed to go further by using an innovative and simple compressive method, which promotes the ionic interactions at the same time that the residual liquid is absorbed, increasing its structural stability and significantly decreasing its acidic environment, being completely neutralized later requiring less amounts of water and cleaning reagents. It is necessary to apply green metrics, such as Atom economy (AE), process mass intensity (PMI), and Environmental factor (*E*-factor), to evaluate how green a process is. This calculation is especially useful when new methods are developed, to demonstrate the environmental impact of generated waste and assess sustainability.[22,23]

The present study aims to provide a deeper understanding of the relationships between biopolymer structure/composition and the rheological mechanical properties in copolymer hydrogels-based formulations (on blending 2 or 3 biopolymers) using natural ionic cross-linking. The developed binary and tertiary polymer hydrogels based on marine biopolymers as collagen (from jellyfish), chitosan (from squid pens), and fucoidan (from brown algae) and characterized regarding morphological and rheological properties.

Results and discussion

Green metrics on scaffolding process

It is of great importance to evaluate the sustainability of newly developed methods. The *E*-factor is a green metrics concept created in the last century to measure the environmental impact through the resource efficiency and the waste generated during synthesis procedures such as chemicals manufacturing, biomaterial process, among others.[24,25] For example, a higher *E*-factor indicates more waste is generated during the process and consequently, a higher negative impact for the environment. Ideally, the *E*-factor needs to be as close to zero as possible.[22] According to this, the *E*-factor for all biomaterials produced, by the newly developed method blending 2 and 3 marine biopolymers, was calculated. The results obtained are very close to zero, between 0.05 to 0.22. For biomaterials composed of only 2 biopolymers the lowest *E*-factor obtained is 0.05 (H_2), and the largest is 0.22 (H_6), while for the biomaterials which blended 3 biopolymers the lowest value obtained is 0.12 (H_{11}) and the highest is 0.17 (H_{10}). All marine biomaterials and structures developed can be considered sustainable and could be produced in large scale since they present a minimal environmental impact.

Molecular weight determination by GPC

The molecular weight, polydispersity and intrinsic viscosity of the marine polymers were determined using gel permeation chromatography (GPC). The obtained data are shown in Table 1.

Molecular weight is an important key for predicting the influence of biopolymers on the mechanical performance of scaffolds due to the impact upon key parameters such as solution viscosity.[14,26–28] The jCOL biopolymer demonstrated high molecular weight, around 260 kDa, in comparison with other collagens.[29–31] In the case of sCHT biopolymers, they also present a higher molecular weight, around 320 kDa, in accordance with the results obtained in our previous work,[20] despite being from different batches. It was associated the presence of

Table 1 The average values of the weight average molecular weight (M_w), the number average molecular weight (M_n), the polydispersity index (M_w/M_n), and the intrinsic viscosity (IV) of the biopolymers used (jCOL, sCHT, and aFUC) to produce the biomaterials

Samples	M_w (kDa)	M_n (kDa)	M_w/M_n	IV (dl g^{-1})
jCOL	258.5 ± 35.6	230.4 ± 27.2	1.12 ± 0.02	2.17 ± 0.03
sCHT	320.8 ± 14.6	151.6 ± 6.4	2.1 ± 0.1	11.2 ± 0.1
aFUC	88.4 ± 8.6	39.8 ± 3.9	1.9 ± 0.1	0.14 ± 0.01

a higher molecular weight to a careful purification procedure as during the washing process higher molecular weight molecules were retained, while smaller ones were eliminated. The aFUC, just like the other natural sources, can demonstrate variations in terms of chemical composition and/or molecular weight, since their characteristics are directly dependent upon factors such as the source, extraction methodology, life cycle, environment, and collection zone.[10,31,32] In this case, fucoidan presented a lower molecular weight, around 120 kDa, when compared with our previous study that used material from a different batch,[20] and with others studies using *Fucus vesiculosus.*[33] Additionally, fucoidan, together with its oligosaccharide, has a growing interest due to their potential health benefits, such as anticoagulant, antitumor, antiviral, anti-inflammatory, wound-healing properties, among others.[32]

Attenuated total reflectance – Fourier transform infrared (ATR-FTIR) spectroscopy

The marine biopolymers and hydrogels, combining two or three components in different concentrations, were analyzed using ATR-FTIR. The respective FTIR spectra are shown in Fig. 1. The spectra depicted in Fig. 1a belongs to collagen from jellyfish (jCOL), which present a typical profile of collagen, highlighting the presence of the amides A, B, I, II, and III.[20,29] The amide A is found at 3299 cm^{-1}, which is associated with N–H stretching vibration, typically seen within a range between 3000–3500 cm^{-1}.[14,34] The presence of this amide indicates the existence of hydrogen bonds, possibly promoted by carbonyl groups present on the peptide chain.[35,36] The amide B was observed at 2935 cm^{-1} (can be detected into the range 3000–2870 cm^{-1}), associated with an asymmetrical stretching of CH_2.[37] The amide I is located between 1650–1635 cm^{-1} that corresponds to the stretching vibration of C═O of the carbonyl groups in proteins.[34,38] This peak it is useful to analyze the secondary structure of the protein since if it appears at lower wavenumber, it can be associated with the denaturation of the protein (loss the triple helix in coiled structure).[39] The peaks of amide II and III found at 1540 cm^{-1} and 1238 cm^{-1}, respectively. These are associated with N–H bending vibration coupled with C–N stretching vibration,[40,41] and N–H deformation and/or C–N stretching vibration.[42,43]

The presence of amides also characterizes the chitosan, and the profile observed in Fig. 1b is similar to the literature.[44] The first band corresponds to N–H stretching vibration, which is associated with intramolecular hydrogen bonding with a peak at 3285 cm^{-1}.[45] The amides I, II, and III appear at 1645, 1549, and 1373 cm^{-1}, corresponds to vibration of C═O and/or N–H, vibration N–H, and C–H, respectively.[46] Additionally, it is possible to observe a broad peak between 1200 cm^{-1} and 950 cm^{-1} that is typically associated with C–O–C and C–O

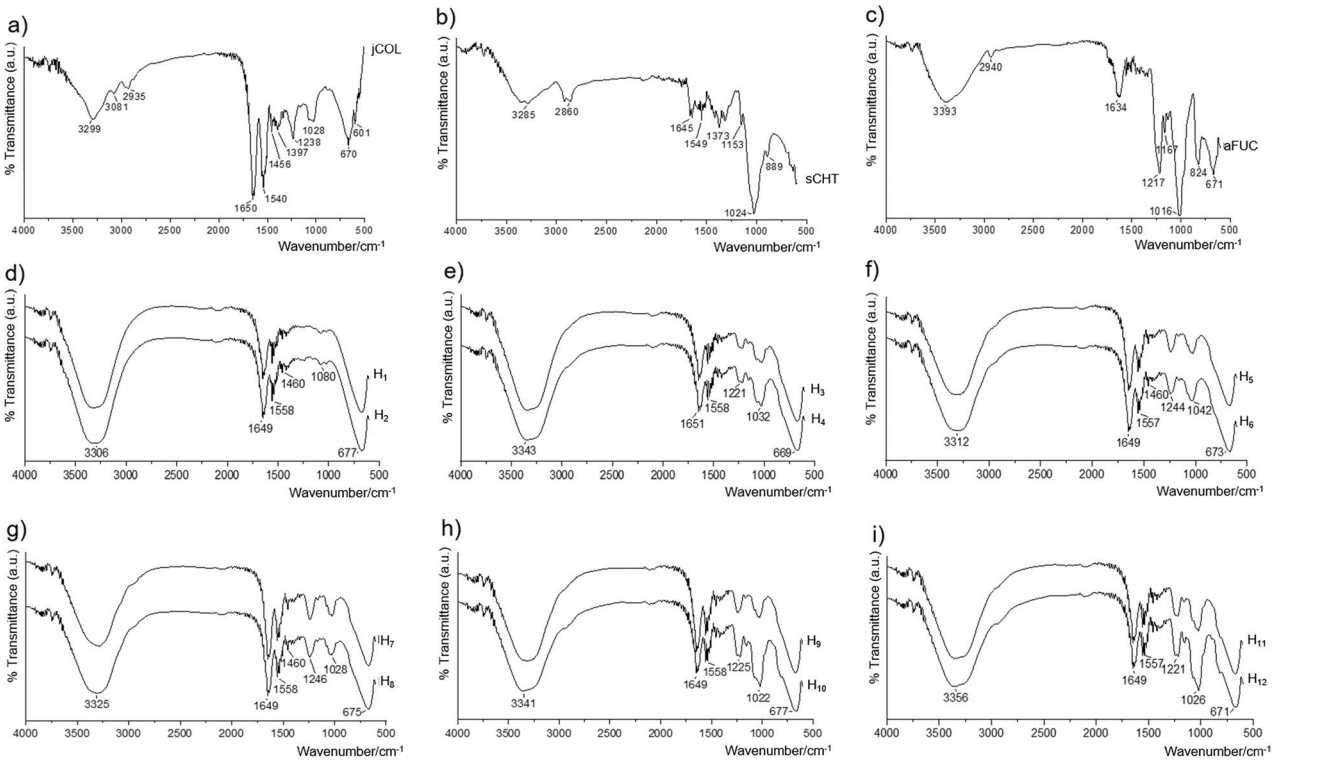

Fig. 1 Attenuated Total Reflectance – Fourier Transform InfraRed (ATR-FTIR) spectra of (a) collagen from jellyfish (jCOL); (b) chitosan from squid pens (sCHT); (c) fucoidan from brown algae (aFUC); (d) hydrogels composed by collagen and chitosan (H_1 and H_2); (e) hydrogels composed by fucoidan and chitosan (H_3 and H_4); (f) and (g) hydrogels composed by collagen and fucoidan (H_5 to H_8); (h) and (i) hydrogels composed by collagen, chitosan, and fucoidan (H_9 to H_{12}). Each hydrogel contains different concentrations of each polymer according to formulations in Table 4 (Materials and methods section).

bonding, related to the bridge stretching of the glucosamine residue.[47]

The fucoidan spectra can be observed in Fig. 1c and is characteristic of a sulfated polymer. However, the number of sulfated groups is directly conditioned to the raw material (species), the life cycle, the environmental conditions and the extraction process used.[32] Nevertheless, fucoidan spectra are generally very similar to those found in the literature.[48,49] The first band centered at 3393 cm^{-1} is accompanied by a peak with less intensity at 2940 cm^{-1}.

These bands are typically attributed to hydrogen-bond O–H stretching vibration[50] and aliphatic C–H,[51] respectively. The next peak found at 1634 cm^{-1} corresponds to the asymmetric stretching of O–C–O vibration, which designates the absorbance of uronic acids.[52] The peak at 1217 cm^{-1} is associated with the presence of sulfate groups, namely S=O stretching.[49,53] The intensity peak at 1016 cm^{-1} corresponds to glycosidic links.[54] Some authors attribute the higher anticancer properties to the types of glycosidic bonds and the contents of sulfate groups present on fucoidan samples.[55] The last two peaks around 824 and 671 cm^{-1} correspond to C–O–S bending vibration of sulfate substituents and to the asymmetric and symmetric O=S=O, which confirmed the presence of sulfates.[53]

From Fig. 1d, it is possible to verify the absence of the signal from sulfate groups, on the range between 1300–700 cm^{-1}, which is coherent with the sample's composition since these two hydrogels (H_1 and H_2) do not contain fucoidan in their formulations. It is also noticed that amide A band is overexpressed by the presence of the biopolymer's collagen and chitosan on the hydrogel's composition. The other hydrogels containing fucoidan revealed the presence of the peak characteristic of sulfate groups. The hydrogels with the same components, but at different concentrations, had FTIR spectra that demonstrate to be similar between them, with some slight differences in some peaks intensity, as on hydrogels H_9 *vs.* H_{10} and H_{11} *vs.* H_{12}, in which the sulfate group peak is more intense when the concentration of fucoidan was higher. In general, the FTIR spectra of hydrogels are similar to the native biopolymers spectra, which indicates no changes in the structures when they are mixed.

Scanning electron microscopy (SEM)

The surface microenvironment of the developed marine scaffolds was observed by scanning electron microscopy, with the respective images shown in Fig. 2a–l. The SEM images were performed to compare the structural morphology of the samples (scaffold networks) obtained from blending 2 or 3 biopolymers. To minimize the potential impact of external interferences, the samples were processed and dried at the same conditions and the reproducibility was tested. Other drying techniques could have been used for this analysis, such as critical point drying (CPD)[56] and hexamethyldisilazane (HMDS),[57] but the purpose of the present study was to assess the differences between samples composition network and not of processing methodologies, including drying. In a first

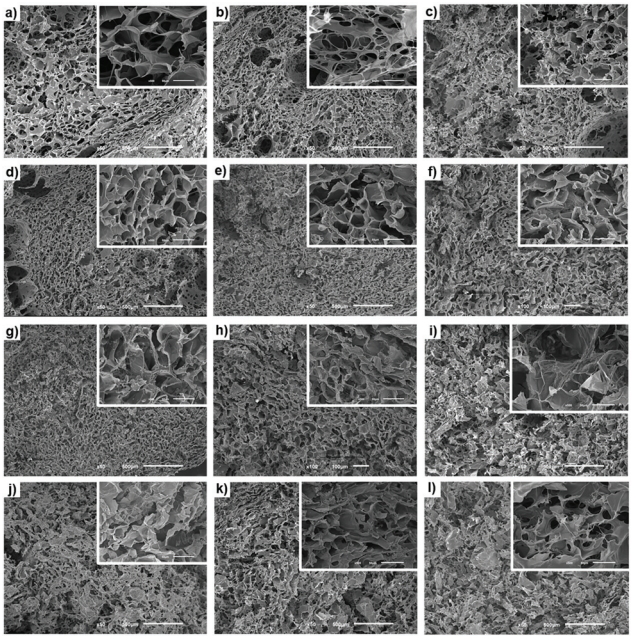

Fig. 2 Scanning electron microscopy (SEM) images of all scaffolds (freeze-dried condition): (a) to (h) (H_1 to H_8, respectively) are related to samples produced by blending two biopolymers, while the images (i) to (l) (H_9 to H_{12}, respectively) are from the biomaterials produced by blending three marine biopolymers. All images at the magnification of ×50/500 μm, ×100/100 μm, and ×500/50 μm.

interpretation, it is noticed a well-defined microstructure with the presence of pores in all structures, though with different pore sizes, mean pore diameter of each combination is shown in Table 2.

These differences are related to the type and concentration of the combined biopolymers. The 2-biopolymer scaffolds presented a larger pore size (around 50 μm to 40 μm) when compared to 3-polymer scaffolds (approximately 30 μm). It was observed that for the structures containing the same polymer composition but with different concentrations (for example H_1 *vs.* H_2 where H_2 contains more collagen than H_1, or H_3 *vs.* H_4 where H_4 contains more fucoidan than H_3), the samples containing a higher concentration of some biopolymer (*e.g.* H_2, H_4, H_6, H_8, H_{10}, and H_{12}) exhibited a pore size smaller than the other samples (*e.g.* H_1, H_3, H_5, H_7, H_9, and H_{11}). This result can be related to the presence of a higher number of

Table 2 Average and standard deviation of the pore size of all marine origin scaffolds

Sample	Mean pore diameter (μm)	Sample	Mean pore diameter (μm)
H_1	45.1 ± 7.2	H_7	36.2 ± 9.4
H_2	41.5 ± 6.8	H_8	28.2 ± 5.8
H_3	43.3 ± 14.2	H_9	31.2 ± 4.4
H_4	34.1 ± 6.9	H_{10}	26.6 ± 8.4
H_5	41.8 ± 7.6	H_{11}	27.1 ± 4.7
H_6	39.7 ± 8.0	H_{12}	23.5 ± 5.5

electrostatic interactions between the charges of each biopolymer, associated with structural strength. Moreover, the materials' stability is more prevalent on 3-polymer hydrogels that are strong enough to support experimental handling, and it is seen on the naked eye. Regarding the 3-polymer hydrogel, the same behavior and similarities in terms of pore size was reported by Carvalho *et al.*[20]

Rheological properties

Oscillatory. Three main groups of experiments were performed regarding the rheological experiments: (i) frequency sweep, (ii) temperature sweep, and (iii) adhesiveness (to stainless steel). It was possible to plot the mechanical spectra (G', G'' *vs.* frequency curves) of each formulation (Fig. 3) from the frequency sweep trials performed at room temperature (25 ± 2 °C).

The storage modulus G' (Pa) describes the elastic (solid) part of the sample's viscoelastic behavior, while the loss modulus G'' (Pa) distinguishes the viscous (liquid) part of the viscoelastic behavior.[58] The oscillatory rheological behavior of different marine hydrogels (from H_1 to H_{12}), shown on Fig. 3, unveiled that all hydrogels exhibited a characteristic viscoelastic behavior with G' higher than G'' almost over the whole tested frequency range. Thus, all the samples tested revealed to have a sol/gel character, as a result of the produced gel internal matrices (physical–chemical interactions or chemical bonds).[3] The storage modulus (G') value at the plateau (between 0.1–1 f/Hz) is denoted as G_e (ref. 3) and was determined to quantify how strong the bonds between the individual molecules of the produced matrices were. In fact, from this value, it is possible to determine the average mesh size (ξ/nm) and the cross-linking density (n_e/mol m^3) of the hydrogels, as described elsewhere.[3] These values were determined from the frequency sweep curves and are shown in Table 3.

G_e points out the variations within the samples, showing a strong gel character for H_{11} (2 times higher) and H_{10} and H_{12} (3 times higher) when compared with the average of the remaining formulations with only two components. Moreover, with the absence of chitosan, samples from H_5 to H_8, the values increased 4 and 5 times with the increase of fucoidan concentration from 5% to 10% and collagen from 3% to 5%, respectively. Besides, the lowest G' values were obtained with the absence of one of these compounds in the presence of the maximum amount of the others, namely for formulations H_2 (no fucoidan, 5% collagen), and H_4 (no collagen, 10% fucoidan). This detail could imply the need for a balance between collagen and fucoidan amounts in the formulations, which could be near the values obtained in the formulations H_{10} and H_{12}, maybe by the possibility to for more bonds between the polymers. Raftery *et al.*,[59] described a similar scaffold that contains 2 biopolymers (collagen from salmon skin and chitosan derived from crustacean shells) and using freeze-drying process. The results demonstrate good mechanical properties, as is the case with our developed materials.

The ξ of the hydrogels varied from 5.2 ± 0.3 nm (H_{10}) to 19.2 ± 1.2 nm (H_2). It is needed to mention that these values are related (by an exponential correlation curve: $y = 1.8e^{0.045x}$, $R^2 = 0.85$) with the pore size presented in Table 3, although they are approximate values obtained using the well-known rubber elastic theory (RET). It is possible to observe that, in general, the mesh size decreased with an increased concentration of the marine components of the hydrogel. This was observed by Karvinen *et al.*[3] However, these authors also observed that adding collagen reduced the mesh size, observed in the results herein shown. In fact, the mesh size or even the pore size (Table 3) are fundamental values for cartilage and drug delivery applications, affecting drug immobilization and diffusion, as well as degradation, swelling and deformation of the hydrogel.[59] Moreover, the effective mesh assigned to cartilage has values between 2 nm and 6 nm,[60] and the hydrogels formerly chosen by their most suitable properties are once again the most promising ones: H_{10} to H_{12}.

Regarding the cross-linking density, this parameter is a relevant factor being reported, for instance, that different levels of cell deformation and heterogeneity may be obtained by varying the cross-linking density in PEG hydrogels.[61] The values herein reported (Table 3) could be achieved by several other approaches, such as from the swelling studies (Flory–Huggins theory), NMR relaxation, diffusion experiments, besides from the modulus plateau from the rheometer or DMA experiments. Thus, the direct comparison is only possible between results obtained for those with the same chemistry base and determined by the same method. Moreover, all those methods provide estimations, more or less close to the accurate value, but are very useful to compare between samples.

The obtained cross-linking density values follow the same trend of the G_e (storage modulus at the frequency sweep plateaux). This is in accordance with the literature since it is expected to exist a proportionality between the cross-link density and the stiffness of the sample.[62]

Oscillatory temp ramp. Temperature sweep experiments were also performed to the hydrogels to understand their thermal behavior under shearing forces (Fig. 4).

The temperature sweeps showed once again the stability of the produced structures, observing only a slight change in behavior from 35 °C to 38 °C up to 50 °C. From these experiments, it was possible to observe that even with the temperature changing, the ratio of G'' to G' (damping factor) did not change significantly, and the samples can be considered stable under these conditions. This performance could be a consequence of the competition between the biopolymers for the constant phase of the system and how the free water is entrapped in a less or more densely packed network.[63]

The damping factor was smaller, and the G_e was higher for the more rigid samples (H_8 and H_{10} to H_{12}) than for the remaining ones. Comparing, for instance, with chitosan containing hydrogels, such as the body temperature-sensitive hydrogels based on chitosan and hyaluronic acid reported by Zhang *et al.*,[64] the stability of the herein exposed hydrogels is remarkable.

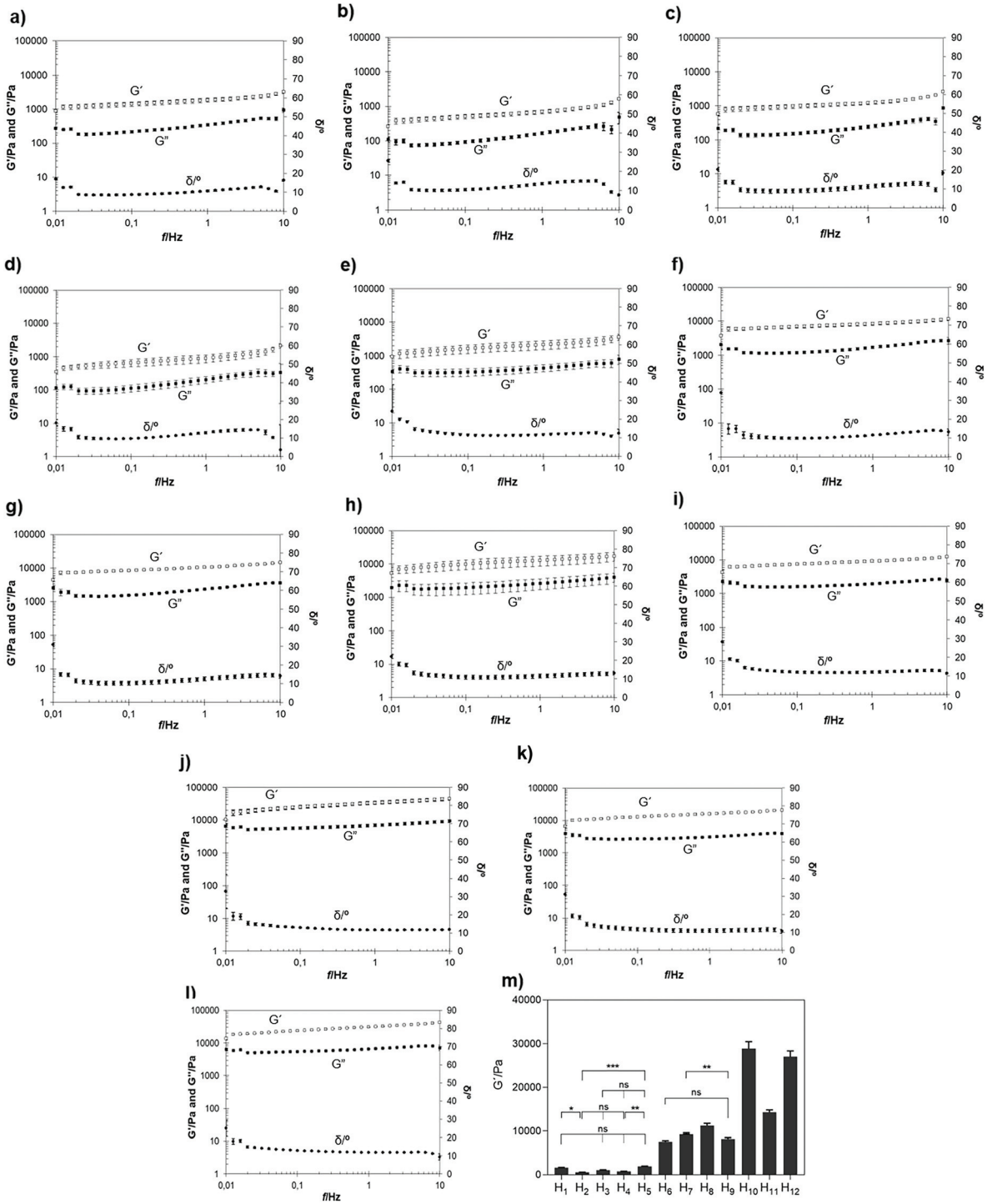

Fig. 3 Oscillatory rheological behavior of different marine origin hydrogels, demonstrated by the elastic modulus (G'), viscous modulus (G''), and phase angle (δ/°) as a function of the frequency: (a) to (l) correspond to H_1 to H_{12}, respectively. Data are reported as the mean of three values from independent experiments ± standard error, (□) G'; (■) G''; and (●) δ/°. (m) Comparison of each marine hydrogel in function of G'/Pa. All samples contain the statistical significance of **** $p < 0.0001$ except those represented with the symbols of * ($p < 0.05$), ** ($p < 0.01$), *** ($p < 0.001$), and ns (no significant).

Adhesivity strength

The adhesivity strength or tackiness is an interesting factor in biomaterials studies to understand their adherence capacity in specific places, as in metal surgical instruments or in (damaged) human tissues, foreseeing their implantation, as a way to avoid dislocations of the biomaterials during and after surgery.[65] Rheology experiments can correlate to the product

Table 3 The average and standard deviation of storage modulus at the plateau (G_e/Pa), average mesh size (ξ/nm) and cross-linking density (n_e/mol m^3) of all marine hydrogel combinations

Sample	G_e/Pa	ξ/nm	n_e/(mol m^{-3})
H_1 (COL^3/CHT^3)	1593 ± 75	13.7 ± 0.7	0.64 ± 0.03
H_2 (COL^5/CHT^3)	580 ± 34	19.2 ± 1.2	0.23 ± 0.01
H_3 (FUC^5/CHT^3)	1077 ± 45	15.6 ± 0.6	0.43 ± 0.02
H_4 (FUC^{10}/CHT^3)	759 ± 43	17.6 ± 1.3	0.31 ± 0.02
H_5 (COL^3/FUC^5)	1882 ± 95	13.0 ± 0.9	0.76 ± 0.04
H_6 (COL^3/FUC^{10})	7527 ± 274	8.2 ± 0.1	3.04 ± 0.11
H_7 (COL^5/FUC^5)	9242 ± 360	7.6 ± 0.5	3.73 ± 0.15
H_8 (COL^5/FUC^{10})	11 230 ± 530	7.2 ± 0.1	4.53 ± 0.21
H_9 (COL^3/CHT^3/FUC^5)	8174 ± 1570	8.0 ± 1.3	3.30 ± 0.63
H_{10} (COL^3/CHT^3/FUC^{10})	28 896 ± 310	5.2 ± 0.3	11.66 ± 0.13
H_{11} (COL^5/CHT^3/FUC^5)	14 283 ± 1356	6.6 ± 0.5	5.76 ± 0.55
H_{12} (COL^5/CHT^3/FUC^{10})	27 012 ± 568	5.3 ± 0.2	10.90 ± 0.23

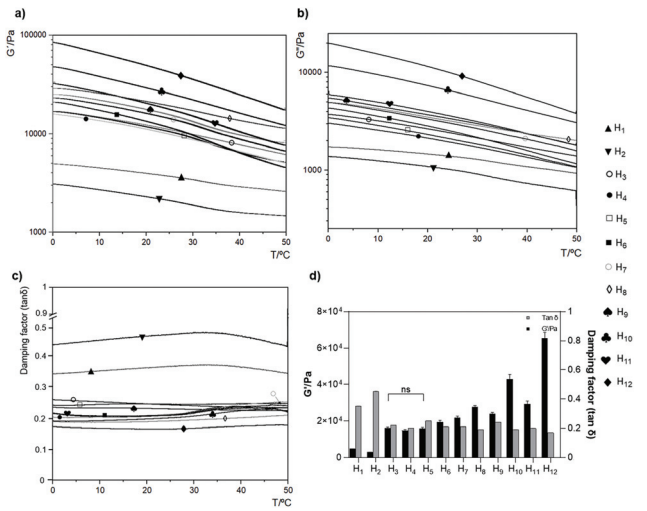

Fig. 4 Oscillatory rheological thermal behavior (single frequency strain-controlled by temperature ramp) of different marine hydrogels, showing the elastic modulus (G'), viscous modulus (G'') and damping factor ($\tan\delta$) as a function of temperature: (a) G', (b) G'', and (c) $\tan\delta$. Values are presented as mean ± S.D. of at least three independent experiments. (d) Comparison of each marine hydrogel in function of G'/Pa (black bar) and the $\tan\delta$ (grey bar), at temperature between 1 and 10 °C (mean and S.D.). In G' data, all samples contain the statistical significance of **** $p < 0.0001$ except that are represented with the symbol of ns (no significant). The $\tan\delta$ data no present statistical significance (ns).

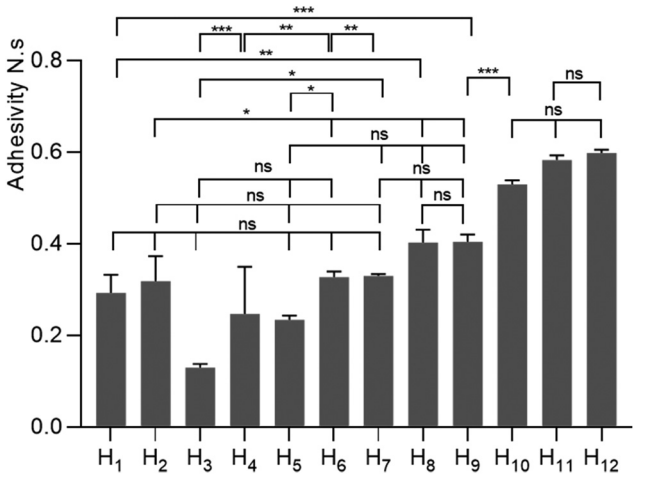

Fig. 5 Comparison of adhesivity strength of all marine hydrogel formulations. Data are presented as mean ± standard error (n = 5), all samples contain statistical significance of $p < 0.0001$ except those represented with the symbols * ($p < 0.05$), ** ($p < 0.01$), *** ($p < 0.001$), and ns (no significant).

tack and peel performance in its final application. Typically, the bio-adhesive material is characterized by their surface tension, the viscosity, and the penetration of the material into the support. The surface tension is a property of the surface of a liquid that allows understanding the resistance of the liquid to an external force, and the viscosity of a fluid is a measure of its resistance to gradual deformation, *i.e.*, the resistance in the spreading.[66] Thus, the adhesive strength behavior of the studied hydrogels was acquired and is shown in Fig. 5.

Currently, there is a growing interest in materials with adhesion properties for clinical practices, that include undegradable materials (*e.g.*, polyurethane and cyanoacrylate), degradable synthetic macromolecules (*e.g.*, poly(vinyl alcohol) and poly(lactic acid)) and the relevant materials for the present study, the biopolymers/polysaccharides as chitosan, but more examples could be given, such as fucoidan, alginic acid, hyaluronic acid, chondroitin sulfate, fibrin,[65,67] collagen/gellatin and mussel foot protein.[68]

The bio-adhesive property is established from biological monomers, such as sugars.[69] Moreover, Citkowska and the coworkers[70] proved that fucoidan has an essential role in this property since it is mostly composed of sulfated fucose and other sugars, such as the uronic acids.[20] The study demonstrates a ratio between the mucoadhesive properties *vs.* biopolymer contents, and it was shown that for a higher bioadhesive property, the concentration of fucoidan in solution needs to be higher as well. Sezer *et al.*[66] also proved this behavior, which demonstrates that the adhesivity enhanced with the addition of fucoidan into gel formulations. However, also depending on the biopolymer-biopolymer interaction, this property of fucoidan can be influenced by the molecular composition of the other polymer when the bonds occur.

The adhesivity properties of chitosan are directly related to several factors, such as the intrinsic viscosity–molecular weight relationship, the deacetylation degree (DD), type of solution that dissolves the polymer, and temperature.[66,71] Typically, with the increase in chitosan molecular weight, there is a rise in the viscosity and subsequently in the adhesivity value.

The collagen adhesivity properties are also related to different factors, such as physic-chemical properties (*e.g.*, surface charge), viscosity, type of collagen, species of origin, animal age, concentration of the sample in solution, the solution type, acid or base solution and temperature.[72,73]

Considering the obtained data, the results are in agreement with what would be expected since it is visible that with the combination of higher concentration of fucoidan or collagen,

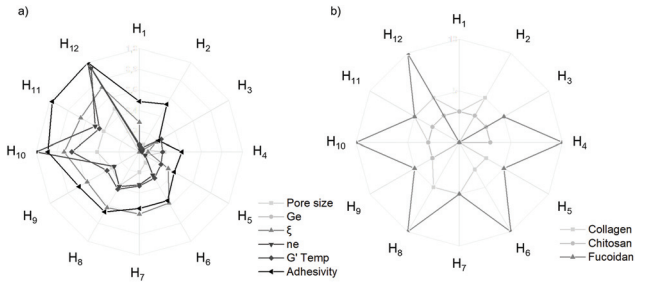

Fig. 6 Radar/spider charts of: (a) the normalized parameters (in arbitrary units) of the studied hydrogels, and (b) their composition (in % w/v).

the hydrogels have better bio-adhesivity properties, for example, H_2 *vs.* H_1 and H_4 *vs.* H_3. Also, the hydrogels that have better adhesivity properties are the hydrogels which have 3-blending polymer (from H_9 to H_{12}). Additionally, the H_8 has demonstrated excellent properties in terms of mechanical and adhesivity properties, which may be due to its higher concentration of collagen and fucoidan.

Comparative evaluation

An overall comparison between the mechanical data obtained and the hydrogels' respective composition was depicted in two spider/radar charts, normalizing the above-obtained results to 0–1 range. Fig. 6 shows both charts, one with the characterization parameters (A), and another with the hydrogel composition (B).

Fig. 6 shows a brief, straightforward, and conclusive comparative examination of the present study results. This type of chart aims to provide an efficient tool to easily correlate all the variables. As foreseen, the superiority of the samples H_{10}, H_{11}, and H_{12} is remarkable and easily noticed by the more external position of their properties (Fig. 6), followed by samples H_7, H_8, and H_9 (Fig. 6A). The reasons for this superiority were already discussed, but a look at chart B reveals that the combination of the three biopolymers was crucial to create a stable biomaterial and to increment their properties. Moreover, the sample H_3 is visibly the weaker sample, which its attributed to the lower concentration of fucoidan and to the absence of collagen in its composition.

Also, when compared with H_4, it is noticed that the presence of a higher concentration of fucoidan only increased the adhesivity properties. Additionally, when comparing the 2 biopolymers hydrogels, the samples that contain collagen (H_1, H_2, H_5 to H_8) had increased mechanical properties, meaning that the presence of chitosan does not seem to have played a significant role in the mechanical properties of these materials. This condition is also noticed when comparing H_9 (3 components system) with H_7 and H_8 (2 components systems with a higher concentration of collagen), showing particularly the same behavior, further reinforcing the idea that the concentration of the polymers is an important factor. However, the presence of certain compounds can obviously be justified by the fact that they add valuable biological attributes for TE.[13]

Materials and methods

Materials

Collagen from Jellyfish (*Rhizostoma pulmo*) (jCOL), kindly supplied by Jellagen Ltd (United Kingdom), Fucoidan from brown algae *Fucus vesiculosus*, aFUC, product: Maritech Fucoidan, FVF2011527 Marinova, Australia was used as received. Chitosan was obtained using a method described in the literature[74] with a deacetylation degree (DD) of 90.1%. Briefly, chitin from squid pens of giant squid (*Dosidicus gigas*) (sCHT) was converted into chitosan using a deacetylation method by an alkaline process, at a ratio of 1 : 10 (w/v), and temperature comprised between 85 to 100 °C, over 2 h.

Marine hydrogel preparation

Initially, the collagen and the chitosan were separately dissolved in acetate buffer (0.15 M NH_4OAc/0.2 M AcOH) around pH 4.75, while the fucoidan was solubilized in ultra-pure water (Milli-Q). The marine biopolymer solutions were mixed using a blender (ultra-turrax T18 overhead Blended, IKA Works Inc., USA) in lower rotations to create homogenous mixtures, avoiding bubbles, using the formulations indicated in Table 4. The resulting solutions were distributed in a 48-well plate, with several layers of filter paper (d = 9 mm) placed on the top of each well, and incubated at a temperature of 37 °C, for approximately 30 minutes. During the incubation time, the filter paper absorbed the residual liquid and compacted the biopolymers, promoting the natural cross-linking (polyelectrolyte interactions) between the polymers. The procedure of the developed hydrogels is illustrated in Fig. 7.

To evaluate if our innovative process of manufacturing the biomaterials is sustainable for the environment, we used the green metrics in the form of a simple calculation of the environmental factor (E-factor), according to the following Sheldon equation[22] (eqn (1)):

$$E\text{-factor} = \frac{(\sum m(\text{raw materials}) + \sum m(\text{reagents}) + \sum m(\text{solvents}) - m(\text{products}))}{m(\text{products})} \quad (1)$$

Gel permeation chromatography (GPC)

The molecular weight and polydispersity index of the collagen (jCOL), fucoidan (aFUC) and chitosan (sCHT) were measured using Malvern Viscotek TDA 305 (gel permeation chromatography) with refractometer (RI-Detector 8110, Bischoff), right and low angle light scattering (L.S.) and viscometer detectors on a set of two types of columns, the NOVEMA and the SUPREMA. NOVEMA was used for cationic polymers, while SUPREMA was used for anionic and neutral polymers.

Table 4 Hydrogel composition prepared by blending 2 or 3 marine origin biopolymers (ratio of each biopolymer in original solution and their distribution percentage after biomaterial formation)

	mg mL^{-1} of polymer in the original solution			
Amount of polymer	Collagen	Chitosan	Fucoidan	Hydrogel abbreviation (100%)
2 bio-polymers	30; (50)	30; (50)	—	H_1 (COL^3/CHT^3)
	50; (62.5)	30; (37.5)	—	H_2 (COL^5/CHT^3)
	—	30; (37.5)	50; (62.5)	H_3 (FUC^5/CHT^3)
	—	30; (23.1)	100; (76.9)	H_4 (FUC^{10}/CHT^3)
	30; (37.5)	—	50; (62.5)	H_5 (COL^3/FUC^5)
	30; (23.1)	—	100; (76.9)	H_6 (COL^3/FUC^{10})
	50; (50)	—	50; (50)	H_7 (COL^5/FUC^5)
	50; (33.3)	—	100; (66.6)	H_8 (COL^5/FUC^{10})
3 bio-polymers	30; (27.3)	30; (27.3)	50; (45.4)	H_9 (COL^3/CHT^3/FUC^5)
	30; (18.8)	30; (18.8)	100; (62.4)	H_{10} (COL^3/CHT^3/FUC^{10})
	50; (38.5)	30; (23.0)	50; (38.5)	H_{11} (COL^5/CHT^3/FUC^5)
	50; (27.8)	30; (16.6)	100; (55.6)	H_{12} (COL^5/CHT^3/FUC^{10})

mg mL^{-1} (w/v) of polymer in the original solution. % w/w of the total polymer mass in hydrogel.

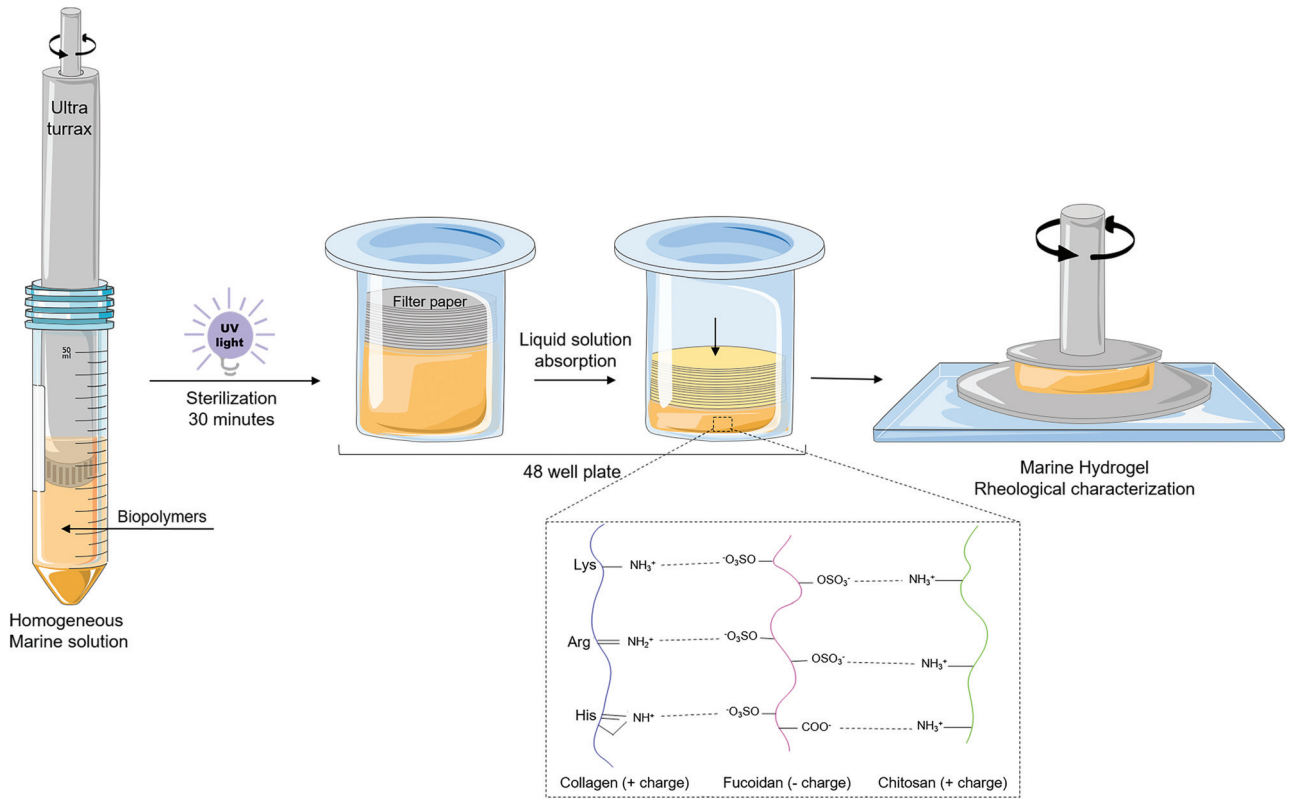

Fig. 7 Schematic representation of (marine origin) hydrogel formation process based in blending of marine origin biopolymers collagen, chitosan and fucoidan, followed by slow removal of excess solvent, under incubation at 37 °C. The ionic electrostatic interactions are promoted between the positively charged groups (protonated amines) of collagens and/or chitosan and the negatively charged groups (*e.g.* ester sulfates and carboxylates) of fucoidan.

The jCOL and sCHT were dissolved (1 mg mL^{-1}) on the eluent with 0.15 M ammonium acetate (NH_4OAc) and 0.2 M acetic acid (AcOH) solution (pH 4.5), and the fucoidan (aFUC) was dissolved in PBS (0.01 M phosphate buffer, 0.0027 M potassium chloride and 0.137 M sodium chloride, pH 7.4, at 25 °C, Sigma-Aldrich) and 0.05% w/v NaN_3. After that, the solutions were filtered through a 0.22 μm membrane to be analyzed by gel permeation chromatography (GPC).

The cationic polymers (jCOL and sCHT) were measured with a NOVEMA column set, composed by a pre-column NOVEMA Max, 10 μm, 8 × 50, NOVEMA Max 30 Å, 10 μm and 2 equivalent columns 8 × 300, NOVEMA Max 1000 Å. The system

was kept at 30 °C. We used the eluent 0.15 M NH_4OAc/0.2 M AcOH buffer (pH 4.5), at 25 °C, (Sigma-Aldrich) at rate of 1 mL min^{-1}. A refractive index increment value (d*n*/d*c*) of 0.18 was used to calculate the absolute molecular weight of all chitosan samples.[75,76]

The anionic polymer (aFUC) was measured with a SUPREMA column set, composed by four columns: pre-column SUPREMA, 5 μm, 8 × 50, SUPREMA 30 Å, 5 μm, 8 × 300, and 2× SUPREMA 1000 Å, 5 μm 8 × 300. The system was kept at 30 °C. We used the eluent 0.15 M NH_4OAc/0.2 M AcOH buffer (pH 4.5), at 25 °C, (Sigma-Aldrich) at rate of 1 mL min^{-1} with both sets of columns, the absolute molecular weight was determined by a calibration of the R.I. and L.S. detectors, using the software Omnisec 5.12 (ViskoteK) with a standard of pullulan with M_n 48.8 kDa and PDI 1.07.

Attenuated total reflectance – Fourier transform infrared (ATR-FTIR) spectroscopy

The FTIR spectra of the marine biopolymers were obtained using a Shimadzu-IR Prestige 21 spectrometer with ATR mode in the spectral region corresponding to 4000–600 cm^{-1}, with a resolution of 2 cm^{-1} as the average of 32 individual scans. The samples were pressed through attenuated total reflectance (ATR) crystal to be analyzed in transmission mode.

Scanning electron microscopy (SEM)

The surface microenvironment of the developed marine scaffolds was observed with a Nova NanoSEM 200 scanning electron (SEM) (JSM-6010LV, JEOL, Tokyo, Japan). The morphology of the samples was analyzed in SEM after fixed on aluminum stubs using a mutual conductive adhesive tape and covered with gold using a Leica EM ACE600 sputter coater. The porosity of the samples was calculated using the image J software, an average of at least ten porous was measured.

Rheological measurements

Rheological properties of the hydrogels were determined using a Kinexus pro+ rheometer (Malvern Instruments, UK), equipped with an upper measurement geometry (8 mm of diameter) and a lower plate pedestal, both in stainless steel (316 grade), and the rSpace software (Malvern Instruments, UK) for the data acquisition.

Firstly, the oscillatory experiments were performed to study the viscoelastic properties of the hydrogels through their mechanical spectra (frequency sweep curves). Linear viscoelastic region (LVER) for the hydrogels was first determined through a strain sweep test (0.01–10%) using a constant frequency (1 Hz) at room temperature (25 °C). This region reveals the range in which the oscillatory experiments can be carried out without damaging the sample structure. Then, the frequency sweep curves were obtained in a range of 0.1 Hz to 10 Hz at 25 °C, using the value of strain (1%) obtained from the LVER.

The thermal behavior (single frequency strain-controlled by temperature ramp) of the marine biomaterials was assessed by a temperature ramp of 0 °C to 50 °C, with the frequency fixed at 1 Hz. The analysis was obtained using an average of at least three experiments.

Additionally, the adhesiveness strength of the hydrogels was measured using the rheometer pull away test. These trials require loading a sample in a typical way (place the sample on the lower plate and lower down the upper geometry to the surface of the sample) and then pulling away the upper plate from the sample at a defined gap speed (1 mm s^{-1}), with 1 N and 2 s of contact force and time, respectively. The area under the force-gap curve was used to determine the adhesion strength. Each experimental condition was repeated at least five times.

The rheological oscillatory experiments can be used to calculate some structural parameter, as the average mesh size and the cross-linking density of the hydrogels.[3] The average mesh size (ξ/nm), is defined as the distance between the cross-linking points, and can be determined from the well-known rubber elastic theory (RET), according to the following eqn (2):

$$\xi = \left(\frac{G' N_A}{RT}\right)^{-1/3} \quad (2)$$

where G' is the storage modulus, N_A is the Avogadro constant (6.022×10^{23}), R is a value of gas constant (8.314 J K^{-1} mol^{-1}), and T is the temperature in Kelvin (25 °C = 298.15 K).[17] The value obtained with these units is taken in meters and then converted into nanometers.

The cross-linking density (n_e/(mol m^{-3}) is designated by the number of elastically active junctions in the network per unit of volume and can also be calculated by RET, following the eqn (3):

$$n_e = \frac{G_e}{RT} \quad (3)$$

where G_e is the plateau value of storage modulus measured by stable frequency sweep test, between 0.1–1 f/Hz.[77]

Statistical analysis

Statistical analysis of rheology results was performed by two-way ANOVA followed by Turkey's *post hoc* test, using GraphPad Prism 8.0.1 (GraphPad Software, Inc., La Jolla, Ca). Differences between the groups with a confidence level of 95% ($p < 0.05$) were considered statistically significant. All results are presented as mean ± standard deviation.

Conclusions

A study of the relationship between the structure/composition and the rheological properties of hydrogel based on blending 2 or 3 marine biopolymers (collagen, chitosan, and fucoidan) was undertaken. In general, the hydrogels containing different blends of the 3 biopolymers demonstrated better mechanical properties in relation to the others. Among the hydrogels composed by two marine origin polymers, the ones with higher polymer concentration showed as well better mechanical properties. Moreover, the data proved that the presence of chito-

san in these hydrogels did not influence significantly their mechanical properties, that are in agreement with the 2-blending hydrogel referred above. The hydrogels also confirmed to have an excellent structural microenvironment to support the cells in future approach, supporting the capacity to facilitate cell migration, since the pore size of the structure is larger than the cell sizes. In general, the developed marine hydrogel systems have excellent potential for biomedical fields as tissue engineering and regenerative medicine approaches, namely for articular cartilage treatment. Moreover, this was achieved by using a green process. As a result, the *E*-factor values obtained for each structure are very close to zero. Therefore, all the structures developed can be considered sustainable and could potentially be scaled up without a negative impact on the environment.

Author contributions

Regarding CRediT taxonomy, the author contributions were: D. N. Carvalho, and C. Gonçalves: Conceptualization; date curation; formal analysis; investigation; methodology; software; visualization and writing – original draft, review & editing. D. S. Williams, and A. Mearns-Spragg: Resources; validation. J. M. Oliveira, R. L. Reis, and T. H. Silva: Conceptualization; supervision; validation; resources; writing – review and editing; funding acquisition.

Conflicts of interest

D. S. Williams, and A. Mearns-Spragg, are Jellagen Ltd employees, manufacturers of jellyfish collagen as used in this research.

Acknowledgements

The authors would like to acknowledge to Portuguese Foundation of Science and Technology (FCT) for a Ph.D. fellowship (D. N. Carvalho) under the scope of the doctoral program Tissue Engineering, Regenerative Medicine and Stem Cells, ref. PD/BD/143044/2018, and for Postdoctoral fellowship (C. Gonçalves), ref. SFRH/BPD/94277/2013. This work has been partially funded by ERDF under the scope of the Atlantic Area Program through project EAPA_151/2016 (BLUEHUMAN). The authors also thank Jellagen Ltd (UK) for the provision of purified jellyfish collagen. The authors would also like to acknowledge Dr Julio Maroto from the Fundación CETMAR and Roi Vilela from PESCANOVA S.A, Spain, for the kind offer of squid pens, and to Lara L. Reys for the initial chitosan extraction process.

Notes and references

1 W. Wang, R. Narain and H. Zeng, Hydrogels, in *Polymer Science and Nanotechnology*, Elsevier, 2020. pp. 203–244.
2 S. K. Das, T. Parandhaman and M. D. Dey, Biomolecule-assisted synthesis of biomimetic nanocomposite hydrogel for hemostatic and wound healing applications, *Green Chem.*, 2021, **23**(2), 629–669.
3 J. Karvinen, T. O. Ihalainen, M. T. Calejo, I. Jonkkari and M. Kellomaki, Characterization of the microstructure of hydrazone crosslinked polysaccharide-based hydrogels through rheological and diffusion studies, *Mater. Sci. Eng., C*, 2019, **94**, 1056–1066.
4 H. D. N. Tran, K. D. Park, Y. C. Ching, C. Huynh and D. H. Nguyen, A comprehensive review on polymeric hydrogel and its composite: Matrices of choice for bone and cartilage tissue engineering, *J. Ind. Eng. Chem.*, 2020, **89**, 58–82.
5 F. Della Sala, M. Biondi, D. Guarnieri, A. Borzacchiello, L. Ambrosio and L. Mayol, Mechanical behavior of bioactive poly(ethylene glycol) diacrylate matrices for biomedical application, *J. Mech. Behav. Biomed. Mater.*, 2020, **110**, 1–9.
6 J. M. Orban, L. B. Wilson, J. A. Kofroth, M. S. El-Kurdi, T. M. Maul and D. A. Vorp, Crosslinking of collagen gels by transglutaminase, *J. Biomed. Mater. Res.*, 2004, **68A**(4), 756–762.
7 A. Oryan, A. Kamali, A. Moshiri, H. Baharvand and H. Daemi, Chemical crosslinking of biopolymeric scaffolds: Current knowledge and future directions of crosslinked engineered bone scaffolds, *Int. J. Biol. Macromol.*, 2018, **107**(Pt A), 678–688.
8 L. Zhang, J. Hu and K. A. Athanasiou, The role of tissue engineering in articular cartilage repair and regeneration, *Crit. Rev. Biomed. Eng.*, 2009, **37**(1–2), 1–57.
9 E. A. Makris, A. H. Gomoll, K. N. Malizos, J. C. Hu and K. A. Athanasiou, Repair and tissue engineering techniques for articular cartilage, *Nat. Rev. Rheumatol.*, 2015, **11**(1), 21–34.
10 T. H. Silva, J. Moreira-Silva, A. L. Marques, A. Domingues, Y. Bayon and R. L. Reis, Marine origin collagens and its potential applications, *Mar. Drugs*, 2014, **12**(12), 5881–5901.
11 F. Subhan, M. Ikram, A. Shehzad and A. Ghafoor, Marine collagen: An emerging player in biomedical applications, *J. Food Sci. Technol.*, 2015, **52**(8), 4703–4707.
12 S. Mantha, S. Pillai, P. Khayambashi, A. Upadhyay, Y. Zhang, O. Tao, *et al.*, Smart hydrogels in tissue engineering and regenerative medicine, *Materials*, 2019, **12**(20), 1–33.
13 B. Hoyer, A. Bernhardt, A. Lode, S. Heinemann, J. Sewing, M. Klinger, *et al.*, Jellyfish collagen scaffolds for cartilage tissue engineering, *Acta Biomater.*, 2014, **10**(2), 883–892.
14 R. O. Sousa, A. L. Alves, D. N. Carvalho, E. Martins, C. Oliveira, T. H. Silva, *et al.*, Acid and enzymatic extraction of collagen from Atlantic cod (*Gadus morhua*) swim bladders envisaging health-related applications, *J. Biomater. Sci., Polym. Ed.*, 2019, **31**(1), 1–18.
15 M. Gelinsky, Biopolymer hydrogel bioinks, in *3D Bioprinting for Reconstructive Surgery*, 2018, pp. 125–136.

16 A. J. Engler, S. Sen, H. L. Sweeney and D. E. Discher, Matrix elasticity directs stem cell lineage specification, *Cell*, 2006, **126**(4), 677–689.
17 P. B. Welzel, S. Prokoph, A. Zieris, M. Grimmer, S. Zschoche, U. Freudenberg, *et al.*, Modulating biofunctional starPEG heparin hydrogels by varying size and ratio of the constituents, *Polymers*, 2011, **3**(1), 602–620.
18 S. Lin, N. Sangaj, T. Razafiarison, C. Zhang and S. Varghese, Influence of physical properties of biomaterials on cellular behavior, *Pharm. Res.*, 2011, **28**(6), 1422–1430.
19 E. Santos, J. L. Pedraz, R. M. Hernandez and G. Orive, Therapeutic cell encapsulation: ten steps towards clinical translation, *J. Controlled Release*, 2013, **170**(1), 1–14.
20 D. N. Carvalho, R. Lopez-Cebral, R. O. Sousa, A. L. Alves, L. L. Reys, S. S. Silva, *et al.*, Marine collagen-chitosan-fucoidan cryogels as cell-laden biocomposites envisaging tissue engineering, *Biomed. Mater.*, 2020, 1–22.
21 A. Vedadghavami, F. Minooei, M. H. Mohammadi, S. Khetani, A. Rezaei, S. Mashayekhan, *et al.*, Manufacturing of hydrogel biomaterials with controlled mechanical properties for tissue engineering applications, *Acta Biomater.*, 2017, **62**, 42–63.
22 R. A. Sheldon, The E factor 25 years on: the rise of green chemistry and sustainability, *Green Chem.*, 2017, **19**(1), 18–43.
23 R. A. Sheldon, Catalysis: The key to waste minimization, *J. Chem. Technol. Biotechnol.*, 1997, **68**, 381–388.
24 A. Garcia-Quintero and M. Palencia, A critical analysis of environmental sustainability metrics applied to green synthesis of nanomaterials and the assessment of environmental risks associated with the nanotechnology, *Sci. Total Environ.*, 2021, **793**, 1–22.
25 A. Moreno, M. Morsali, J. Liu and M. H. Sipponen, Access to tough and transparent nanocomposites via Pickering emulsion polymerization using biocatalytic hybrid lignin nanoparticles as functional surfactants, *Green Chem.*, 2021, **23**(8), 3001–3014.
26 H. J. Cho, C. S. Ki, H. Oh, K. H. Lee and I. C. Um, Molecular weight distribution and solution properties of silk fibroins with different dissolution conditions, *Int. J. Biol. Macromol.*, 2012, **51**(3), 336–341.
27 E. Amiri, M. Rahmaninia and A. Khosravani, Effect of chitosan molecular weight on the performance of chitosan-silica nanoparticles system in recycled pulp, *Bioresources*, 2019, **14**(4), 7687–7701.
28 C. F. C. João, A. T. Kullberg, J. C. Silva and J. P. Borges, Chitosan inverted colloidal crystal scaffolds: Influence of molecular weight on structural stability, *Mater. Lett.*, 2017, **193**, 50–53.
29 F. F. Felician, R. H. Yu, M. Z. Li, C. J. Li, H. Q. Chen, Y. Jiang, *et al.*, The wound healing potential of collagen peptides derived from the jellyfish Rhopilema esculentum, *Chin. J. Traumatol.*, 2019, **22**(1), 12–20.
30 X. Cheng, Z. Shao, C. Li, L. Yu, M. A. Raja and C. Liu, Isolation, Characterization and evaluation of collagen from jellyfish Rhopilema esculentum Kishinouye for use in hemostatic applications, *PLoS One*, 2017, **12**(1), 1–21.
31 N. M. H. Khong, F. M. Yusoff, B. Jamilah, M. Basri, I. Maznah, K. W. Chan, *et al.*, Improved collagen extraction from jellyfish (Acromitus hardenbergi) with increased physical-induced solubilization processes, *Food Chem.*, 2018, **251**, 41–50.
32 D. N. Carvalho, A. R. Inácio, R. O. Sousa, R. L. Reis and T. H. Silva, Seaweed polysaccharides as sustainable building blocks for biomaterials in tissue engineering, in *Sustainable Seaweed Technologies*, ed. M. D. Torres, S. Kraan and H. Dominguez, 2020, pp. 543–587.
33 C. Oliveira, S. Granja, N. M. Neves, R. L. Reis, F. Baltazar, T. H. Silva, *et al.*, Fucoidan from Fucus vesiculosus inhibits new blood vessel formation and breast tumor growth in vivo, *Carbohydr. Polym.*, 2019, **223**, 115034–115044.
34 R. O. Sousa, E. Martins, D. N. Carvalho, A. L. Alves, C. Oliveira, A. R. C. Duarte, *et al.*, Collagen from Atlantic cod (Gadus morhua) skins extracted using CO_2 acidified water with potential application in healthcare, *J. Polym. Res.*, 2020, **27**(3), 1–9.
35 F. Casanova, M. A. Mohammadifar, M. Jahromi, H. O. Petersen, J. J. Sloth, K. L. Eybye, *et al.*, Physico-chemical, structural and techno-functional properties of gelatin from saithe (Pollachius virens) skin, *Int. J. Biol. Macromol.*, 2020, **156**, 918–927.
36 W. K. Song, D. Liu, L. L. Sun, B. F. Li and H. Hou, Physicochemical and biocompatibility properties of type I collagen from the skin of Nile Tilapia (Oreochromis niloticus) for biomedical applications, *Mar. Drugs*, 2019, **17**(3), 1–14.
37 Y. Tang, S. Jin, X. Li, X. Li, X. Hu, Y. Chen, *et al.*, Physicochemical properties and biocompatibility evaluation of collagen from the skin of giant croaker (Nibea japonica), *Mar. Drugs*, 2018, **16**(7), 1–11.
38 K. Muthumari, M. Anand and M. Maruthupandy, Collagen extract from marine finfish scales as a potential Mosquito Larvicide, *Protein J.*, 2016, **35**(6), 391–400.
39 E. Jeevithan, B. Bao, Y. Bu, Y. Zhou, Q. Zhao and W. Wu, Type II collagen and gelatin from silvertip shark (Carcharhinus albimarginatus) cartilage: isolation, purification, physicochemical and antioxidant properties, *Mar. Drugs*, 2014, **12**(7), 3852–3873.
40 J. C. Silva, A. A. Barros, I. M. Aroso, D. Fassini, T. H. Silva, R. L. Reis, *et al.*, Extraction of collagen/gelatin from the marine demosponge chondrosia reniformis (Nardo, 1847) using water acidified with carbon dioxide – Process optimization, *Ind. Eng. Chem. Res.*, 2016, **55**(25), 6922–6930.
41 Z. Barzideh, A. A. Latiff, C.-Y. Gan, S. Benjakul and A. A. Karim, Isolation and characterisation of collagen from the ribbon jellyfish (Chrysaorasp.), *Int. J. Food Sci. Technol.*, 2014, **49**(6), 1490–1499.
42 M. Atef, S. M. Ojagh, A. M. Latifi, M. Esmaeili and C. C. Udenigwe, Biochemical and structural characterization of sturgeon fish skin collagen (Huso huso), *J. Food Biochem.*, 2020, 1–10.

43 S. Tamilmozhi, A. Veeruraj and M. Arumugam, Isolation and characterization of acid and pepsin-solubilized collagen from the skin of sailfish (Istiophorus platypterus), *Food Res. Int.*, 2013, **54**(2), 1499–1505.
44 J. N. I. Balitaan, J. M. Yeh and K. S. Santiago, Marine waste to a functional biomaterial: Green facile synthesis of modified-beta-chitin from Uroteuthis duvauceli pens (gladius), *Int. J. Biol. Macromol.*, 2020, **154**, 1565–1575.
45 M. S. Yusharani, Stenley, Harmami, I. Ulfin and Y. L. Ni'mah, Synthesis of water-soluble chitosan from squid pens waste as raw material for capsule shell: temperature deacetylation and reaction time, *IOP Conf. Ser.: Mater. Sci. Eng.*, 2019, **509**, 1–11.
46 A. Singh, S. Benjakul and T. Prodpran, Ultrasound–assisted extraction of chitosan from squid pen: Molecular characterization and fat binding capacity, *J. Food Sci.*, 2019, **84**(2), 224–234.
47 H. Salehizadeh, E. Hekmatian, M. Sadeghi and K. Kennedy, Synthesis and characterization of core-shell Fe3O4-gold-chitosan nanostructure, *J. Nanobiotechnol.*, 2012, **10**(3), 1–7.
48 A. Beratto-Ramos, C. Agurto-Munoz, J. P. Vargas-Montalba and R. D. P. Castillo, Fourier-transform infrared imaging and multivariate analysis for direct identification of principal polysaccharides in brown seaweeds, *Carbohydr. Polym.*, 2020, **230**, 1–10.
49 E. Hernández-Garibay, J. A. Zertuche-González and I. Pacheco-Ruiz, Sulfated polysaccharides (fucoidan) from the brown seaweed Silvetia compressa (J. Agardh) E. Serrão, T.O. Cho, S.M. Boo & Brawley, *J. Appl. Phycol.*, 2019, **31**(6), 3841–3847.
50 R. Artemisia, A. K. Nugroho, E. P. Setyowati and R. Martien, The properties of brown marine algae Sargassum turbinarioides and Sargassum ilicifolium collected from Yogyakarta, Indonesia, *Indones. J. Pharm.*, 2019, **30**(1), 43–51.
51 S. Palanisamy, M. Vinosha, M. Manikandakrishnan, R. Anjali, P. Rajasekar, T. Marudhupandi, *et al.*, Investigation of antioxidant and anticancer potential of fucoidan from Sargassum polycystum, *Int. J. Biol. Macromol.*, 2018, **116**, 151–161.
52 A. F. Hifney, M. A. Fawzy, K. M. Abdel-Gawad and M. Gomaa, Industrial optimization of fucoidan extraction from Sargassum sp. and its potential antioxidant and emulsifying activities, *Food Hydrocolloids*, 2016, **54**, 77–88.
53 N. Nunes, G. P. Rosa, S. Ferraz, M. C. Barreto and M. A. A. P. de Carvalho, Fatty acid composition, TLC screening, ATR-FTIR analysis, anti-cholinesterase activity, and in vitro cytotoxicity to A549 tumor cell line of extracts of 3 macroalgae collected in Madeira, *J. Appl. Phycol.*, 2019, **32**(2), 759–771.
54 C.-Y. Wang and Y.-C. Chen, Extraction and characterization of fucoidan from six brown macroalgae, *J. Mar. Sci. Technol.*, 2016, **24**(2), 319–328.
55 Y. Zhao, Y. Zheng, J. Wang, S. Ma, Y. Yu, W. L. White, *et al.*, Fucoidan extracted from Undaria pinnatifida: Source for nutraceuticals/functional foods, *Mar. Drugs*, 2018, **16**(9), 1–17.
56 H. Radhouani, S. Correia, C. Goncalves, R. L. Reis and J. M. Oliveira, Synthesis and characterization of biocompatible methacrylated kefiran hydrogels: Towards tissue engineering applications, *Polymers*, 2021, **13**(8), 1–16.
57 A. G. Pogorelov and I. I. Selezneva, Evaluation of collagen gel microstructure by scanning electron microscopy, *Cell Technol. Biol. Med.*, 2010, **150**(1), 153–156.
58 A.I Barzic and S. Ioan, Viscoelastic behavior of liquid-crystal polymer in composite systems, in *Viscoelastic and Viscoplastic Materials*, 2016, pp. 35–52.
59 R. M. Raftery, *et al.*, Multifunctional biomaterials from the sea: Assessing the effects of chitosan incorporation into collagen scaffolds on mechanical and biological functionality, *Acta Biomater.*, 2016, **43**, 160–169.
60 J. M. Urueña, A. A. Pitenis, R. M. Nixon, K. D. Schulze, T. E. Angelini and W. G. Sawyer, Mesh size control of polymer fluctuation lubrication in gemini hydrogels, *Biotribology*, 2015, **1–2**, 24–29.
61 S. J. Bryant, T. T. Chowdhury, D. D. Lee, D. L. Bader and K. A. Anseth, Crosslinking density influences chondrocyte metabolism in dynamically loaded photocrosslinked poly (ethylene glycol) hydrogels, *Ann. Biomed. Eng.*, 2004, **32**(3), 407–417.
62 G. Hoti, F. Caldera, C. Cecone, R. Pedrazzo, A. A. Anceschi, S. L. Appleton, *et al.*, Effect of the cross-linking density on the swelling and rheological behavior of ester-bridged beta-cyclodextrin nanosponges, *Materials*, 2021, **14**(3), 478–498.
63 B. Simionescu, S. A. Ibanescu, M. Danu, I. Rotaru and C. Ibanescu, Rheology of gelatin-starch systems I, Influence of system composition, *Rev. Chim.*, 2013, **64**(8), 909–913.
64 W. Zhang, X. Jin, H. Li, R.-r. Zhang and C.-w. Wu, Injectable and body temperature sensitive hydrogels based on chitosan and hyaluronic acid for pH sensitive drug release, *Carbohydr. Polym.*, 2018, **186**, 82–90.
65 C. Shi, X. Chen, Z. Zhang, Q. Chen, D. Shi and D. Kaneko, Mussel inspired bio-adhesive with multi-interactions for tissue repair, *J. Biomater. Sci., Polym. Ed.*, 2020, **31**(4), 491–503.
66 A. D. Sezer, *et al.*, Preparation of fucoidan-chitosan hydrogel and its application as burn healing accelerator on rabbits, *Biol. Pharm. Bull.*, 2008, **31**(12), 2326–2333.
67 Z. Deng, Y. He, Y. J. Wang, Y. Zhao and L. Chen, Chondroitin sulfate hydrogels based on electrostatic interactions with enhanced adhesive properties: exploring the bulk and interfacial contributions, *Soft Matter*, 2020, **16**(26), 6128–6137.
68 S. A. Mian and Y. Khan, *The Adhesion Mechanism of Marine Mussel Foot Protein: Adsorption of L-Dopa on-and-Cristobalite Silica Using Density Functional Theory*, 2017, vol. 2017.
69 J.D Mathias, M. Grédiac and P. Michaud, *Bio-based adhesives. Biopolymers and Biotech Admixtures for Eco-Efficient Construction Materials*, 2016. pp. 369–385.
70 A. Citkowska, M. Szekalska and K. Winnicka, Possibilities of fucoidan utilization in the development of pharmaceutical dosage forms, *Mar. Drugs*, 2019, **17**(8), 1–20.

71 J. S. Ahn, H. K. Choi and C. S. Cho, A novel mucoadhesive polymer prepared by template polymerization of acrylic acid in the presence of chitosan, *Biomaterials*, 2001, **22**, 923–928.
72 J.C. Suárez, Bioadhesives, in *Handbook of Adhesion Technology*, 2011. pp. 1385–1408.
73 V. Singh, A. Misra, R. Parthasarathy, Q. Ye and P. Spencer, Viscoelastic properties of collagen-adhesive composites under water-saturated and dry conditions, *J. Biomed. Mater. Res., Part A*, 2015, **103**(2), 646–657.
74 L. L. Reys, S. S. Silva, J. M. Oliveira, S. G. Caridade, J. F. Mano, T. H. Silva, *et al.*, Revealing the potential of squid chitosan-based structures for biomedical applications, *Biomed. Mater.*, 2013, **8**(4), 1–11.
75 P. Sorlier, C. Rochas, I. Morfin, C. Viton and A. Domard, Light scattering studies of the solution properties of chitosans of varying degrees of acetylation, *Biomacromolecules*, 2003, **4**, 1034–1040.
76 B. E. Christensen, I. M. N. Vold and K. M. Vårum, Chain stiffness and extension of chitosans and periodate oxidised chitosans studied by size-exclusion chromatography combined with light scattering and viscosity detectors, *Carbohydr. Polym.*, 2008, **74**(3), 559–565.
77 R. Suriano, G. Griffini, M. Chiari, M. Levi and S. Turri, Rheological and mechanical behavior of polyacrylamide hydrogels chemically crosslinked with allyl agarose for two-dimensional gel electrophoresis, *J. Mech. Behav. Biomed. Mater.*, 2014, **30**, 339–346.